

See discussions, stats, and author profiles for this publication at: <https://www.researchgate.net/publication/268978158>

Enhancement of Two-Photon Absorption Cross Section in CdSe Quantum Rods

ARTICLE *in* THE JOURNAL OF PHYSICAL CHEMISTRY C · AUGUST 2014

Impact Factor: 4.77 · DOI: 10.1021/jp501843g

CITATIONS

2

READS

33

4 AUTHORS, INCLUDING:



[Janusz Szeremeta](#)

Wroclaw University of Technology

13 PUBLICATIONS 117 CITATIONS

[SEE PROFILE](#)



[Dominika Wawrzynczyk](#)

Wroclaw University of Technology

29 PUBLICATIONS 227 CITATIONS

[SEE PROFILE](#)



[Marek Samoc](#)

Wroclaw University of Technology

384 PUBLICATIONS 6,270 CITATIONS

[SEE PROFILE](#)

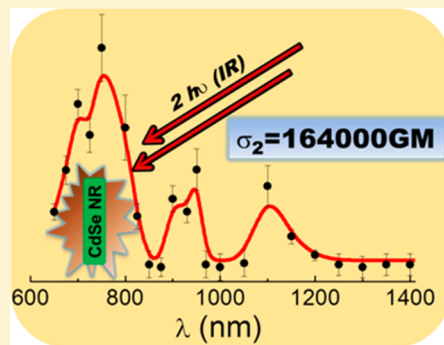
Enhancement of Two-Photon Absorption Cross Section in CdSe Quantum Rods

Marcin Nyk, Janusz Szeremeta, Dominika Wawrzynczyk, and Marek Samoc*

Institute of Physical and Theoretical Chemistry, Wroclaw University of Technology, 50-370 Wroclaw, Poland

S Supporting Information

ABSTRACT: Nonlinear optical properties of semiconducting CdSe quantum rods (QRs), with three various aspect ratios, were examined in a wide wavelength range using femtosecond Z-scan technique. The two-photon absorption cross section σ_2 was found to be as large as 164 000 GM at the wavelength of 750 nm: about 4 times larger than that expected for CdSe quantum dots of the same mass. On the basis of the obtained dispersion of the two-photon absorption cross section, we have selected wavelength ranges for optimal excitation of two-photon-induced emission. We have also studied the luminescence kinetics using degenerate pump–probe and time-correlated single-photon counting techniques. A strong influence of semiconducting CdSe rods morphology on their steady-state and time-resolved optical properties was found.



INTRODUCTION

The use of semiconductor nanocrystals usually referred to as quantum dots (QDs) as luminescence probes for numerous biological¹ and optoelectronic applications² has become an area of intense research over the past years. QDs offer several advantages over organic dyes, including increased brightness, stability against photobleaching, excitation within a broad spectral range, and narrow, symmetric emission spectrum.³ On the other hand, it is known that the formation of organized one-dimensional (nanorods, nanowires, nanotubes),⁴ two-dimensional (triangles, plates, and sheets),⁵ and three-dimensional (pyramids, stars, nanocages)⁶ arrays of anisotropic nanoparticles made of various materials can bring novel properties into the resulting systems, which are quite different from the properties of an individual particle with isotropic zero-dimensional (sphere) morphology.⁷ For example, a slight change in particle geometry can produce great changes in the surface plasmon peak position of metallic gold nanorods,⁸ which can hardly be achieved in the spherical nanosystems through a similar change in diameter. Recently, CdSe quantum rods (QRs) have been shown to possess several interesting optical features comparing to well-known standard CdSe QDs, including those of aspect ratio dependent linearly polarized emission⁹ and sharp emission line with broad excitation and emission color control by rod dimension.¹⁰ An interesting, and only little examined, feature of CdSe QRs is their nonlinear optical (NLO) properties. Up to date, only a small number of authors have reported femtosecond measurements on colloidal semiconducting QRs, and the data were mostly limited to a few discrete wavelengths.^{10,11} In general, different kinds of inorganic materials with optimized nonlinear absorption are needed for numerous applications including those where the nonlinear absorption is used to excite luminescence (e.g., in

two-photon fluorescence microscopy) as well as those where no light emission is required (e.g., optical power limiting). For example, polarization fluorescence microscopy was used to study the nature of the emission and nonlinear absorption dipole of single CdSe/ZnS QRs, where nonlinear excitation showed a sharp angular dependence fully consistent with the predicted two-photon absorption process.¹² A number of previous studies concerning the NLO properties measured at a single wavelength were carried out, in order to get an insight into features of semiconductor QDs other materials¹³ relevant to their interactions with short pulse lasers. However, it is extremely important to characterize the NLO factors, i.e., the nonlinear absorption coefficient and nonlinear refractive index, in a wide wavelength range to find the optimal values of the parameters.¹⁴ Lately, various theories have been proposed for describing the nature of the two-photon absorption (2PA) in colloidal system with quantum dots.^{15,16} The theoretical results considering the mixing of the hole bands obtained from $k \cdot p$ theory explain the experimental data quite well except for the smallest dots. However, this theory is still not capable of predicting the 2PA spectrum at the highest energies.¹⁵ Feng et al.¹⁶ presented a theoretical investigation of two-photon absorption in semiconductor nanomaterials based on a four-band model under effective mass approximation. They found theoretically that lower degree of symmetry of nanocrystals increases the two-photon cross section, where this effect is more sensitive to the lateral size than the longitudinal. Additionally, for better insight into time dependence of both linear and nonlinear optical processes in QRs, the use of

Received: February 21, 2014

Revised: June 24, 2014

Published: July 9, 2014



ultrafast time-resolved optical pump–probe spectroscopy is required. This technique has been used to probe energy relaxation in the excited state manifold on a time scale of femtoseconds to nanoseconds.¹⁷ Ultrafast experimental techniques were also used to probe optical gain, charge transfer, ionization dynamics, carrier multiplication, and the other dynamical processes.¹⁸

The aim of this paper is to assess NLO properties of CdSe QRs, using femtosecond Z-scan and pump–probe techniques, for potential applications in nanophotonics and bioimaging. The current work follows a similar study performed by us recently, where we investigated NLO properties of spherical CdSe¹⁹ and CdS²⁰ QDs using wide-wavelength range low-repetition rate femtosecond Z-scan measurements.

EXPERIMENT

Materials and Synthesis. Cadmium oxide (CdO, 99.99%), selenium powder, tributylphosphine (TBP), trioctylphosphine (TOP), 99% trioctylphosphine oxide (TOPO), tetradecylphosphonic acid (TDPA), and technical grade 1-octadecene (ODE) were purchased from Sigma-Aldrich. Methanol, chloroform, and acetone were purchased from POCH S.A. (Poland).

CdSe QRs were synthesized according to protocol described by Peng et al.²¹ Synthesis was carried out under a Schlenk vacuum-gas line. We applied a quasi-one-pot protocol which includes aging of the Cd–TDPA complex in TOPO. Although Peng et al. have not explained clearly why aging of the precursor promotes anisotropic growth of the QRs, their results show a great improvement of the length-to-width aspect ratio upon aging. The reaction progress with and without Cd precursor aging was monitored with UV–vis spectroscopy, and the results showed that during the synthesis with aged precursor less nuclei centers are formed at the beginning of the synthesis, right after the Se precursor injection, and the concentration of CdSe molecules throughout the synthesis is higher. The authors of ref 21 infer that stable CdSe concentrations and the small amount of nuclei in the case of the quasi-one-pot synthesis promote the formation of the rods.

In a typical synthesis 0.205 g of CdO was mixed with 0.893 g of TDPA and 2.903 g of TOPO in a three-neck round-bottom flask and heated. At ca. 120 °C the reaction flask was evacuated and purged with nitrogen three times. At 320 °C the brown solution became colorless, indicating complete dissolution of CdO. The reaction mixture was cooled to room temperature and left overnight for aging. Next 2.287 g of TOPO was added to aged Cd-TDPA in TOPO and heated again to 320 °C, repeating the process of degassing and purging with nitrogen of the mixture. 0.253 g of 25% w/w Se-TBP solution was prepared and mixed with 1.447 g of TOP and 0.3 g of toluene. At 320 °C the selenium precursor was injected to the cadmium solution with a syringe by the septa closing the neck of the flask. The temperature dropped to 300 °C and was maintained at that level during the reaction time. The color of the reaction mixture changed to deep red; portions of the solution were withdrawn with a syringe after 30, 20, and 10 min, and the obtained CdSe QRs will be consequently named in the text as CS1, CS2, and CS3, respectively. CdSe QRs were precipitated with methanol and centrifuged at 10 000 rpm for 10 min. The resulting sludge was dissolved in chloroform.

Characterization Methods. UV–vis absorption spectra were obtained with a JASCO V670 spectrophotometer, and steady-state fluorescence spectra were recorded with a Hitachi F-4500 spectrofluorometer. Transmision electron microscopy

(TEM) pictures, selected area diffraction (SEAD), and energy dispersive spectroscopy (EDS) were obtained on a FEI Tecnai G² 20 X-TWIN equipped with an EDAX X-ray microanalyzer.

NLO measurements were performed using a femtosecond laser system consisting of a Quantronix Integra-C Ti:sapphire regenerative amplifier, which produces ~130 fs, 800 nm pulses with 1 kHz repetition rate and 1 mJ energy/pulse, pumping a Quantronix Palitra-FS optical parametric amplifier (OPA), the wavelength being tuned in the range from 550 to 1600 nm. Samples for Z-scan measurements were prepared in 1 mm thick, sealed, glass cuvettes. Concentration of the prepared samples was estimated through gravimetric analysis after evaporating solvent from a certain amount of the solution. Concentrations of the samples were 1.6, 2.5, and 1.7 mg/mL for CS1, CS2, and CS3, respectively. Details of the experiment were described elsewhere.^{19,20,22} In our typical routine the sample was scanned through the focus of a laser beam, which was then split into two, two photodiodes being used for the monitoring of the transmitted power. ~1 mm pinhole which transmitted only the center of the beam was placed before the first detector to measure the closed-aperture (CA) signal, while the second detector collected the whole beam to give the open-aperture (OA) signal. At each wavelength the scans of the investigated CdSe QRs samples were preceded by scans of a 4.66 mm thick silica glass plate used as a reference and a cuvette with pure solvent, the latter being used in order to eliminate the contributions of the cuvette walls and the solvent itself to the signals.²² The laser beam was focused to provide a spot size in the range $w_0 \approx 50\text{--}80 \mu\text{m}$, ensuring that the Rayleigh range $z_0 = \pi w_0^2/\lambda$ was always larger than the total thickness of the sample ($\approx 3 \text{ mm}$, which includes two glass walls and the solution inside the cell) or the silica plate ($\approx 4.7 \text{ mm}$). The transmittance curves corresponding to CA and OA Z-scan were fitted using expressions derived by Sheik-Bahae²³ and taking into account the amendments to the theory,^{24,25} which include the contribution of higher order nonlinear processes. This allowed to calculate the real and imaginary part of the complex third-order susceptibility $\chi^{(3)}$ of the solutions which were then converted into the NLO data referring to individual QRs. To compare the strength of the nonlinear absorbance of the CdSe QRs with other nonlinear materials, we have calculated and presented the results as dispersion of the multiphoton absorption cross section (σ_2 and σ_3 , where three-photon behavior was observed) in the whole investigated spectral range and computed the theoretical two- and three-photon absorption cross sections of the individual species of the substance, which in this case was a single CdSe QR.^{14,19,20}

Fluorescence intensity decays were obtained by time-correlated single photon counting (TCSPC) measurements, performed on an IBH time-resolved spectrophotometer (IBH Consultants, Scotland, UK) at 300 K on excitation with a 1.2 ns pulsed laser diode at 460 nm. Fluorescence lifetimes were estimated by fitting the decay data using an interactive deconvolution procedure based on Marquardt algorithm with software supplied by IBH. The kinetics of the excited state absorption was measured using degenerate transient absorption (DTA). The detailed scheme of the experimental setup is presented in Figure S1. We chose two wavelengths—560 nm (~90 μJ) and 800 nm (~150 μJ)—to work in either one-photon or two-photon absorption regime. The laser beam from the OPA was divided into two. The probing beam was attenuated and directed straight to the sample while the pump beam was passed through a motorized delay line and an optical

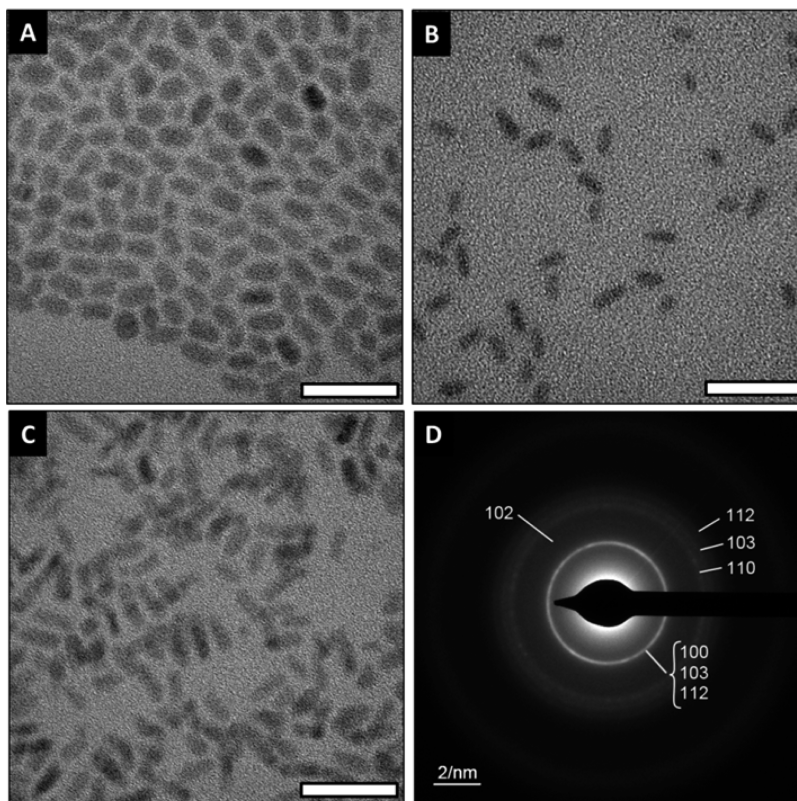


Figure 1. TEM images of CdSe QRs: (a) CS3, (b) CS2, (c) CS1, and (d) representative SAED micrographs (scale bar 30 nm).

chopper. Both beams were focused and intersected at the sample. We monitored the transmission of the probing beam while the optical path of the pump beam was being shortened by moving the delay line stage. Changes of the intensity of the probing beam induced by chopped pump were measured with a lock-in amplifier (Signal Recovery Model 7270). The same samples preparations as for the Z-scan measurements were used for the pump–probe experiments. Additionally, for 800 nm we monitored the autocorrelation signal through second harmonic generation (SHG) in order to measure the pulse length. A BBO crystal cut for frequency doubling of 800 nm light was placed in the setup instead of the sample. When both pulses were coming at the same time, we observed an additional blue spot appearing in the middle between pump and probe beams due to SHG involving the photons from both beams.

RESULTS AND DISCUSSION

TEM images in Figure 1a–c show morphology of the obtained CS1, CS2, and CS3 CdSe QRs. By analyzing the pictures, we determined the average sizes of the CdSe QRs and the aspect ratios (Table 1). From the performed calculations it is evident

that prolonging the reaction time resulted in increase in both CdSe QRs size and the aspect ratio. From the SAED pattern (Figure 1d) the crystallographic structure of a representative CdSe QR was identified as wurtzite.²⁶ Density of bulk CdSe wurtzite and the calculated mean sizes of individual CdSe QRs were used to calculate the molar mass of a single CdSe QR. This value is necessary to calculate the NLO parameters, and appropriate merit factors for quantitative comparisons between different types of QRs and QRs with QDs. The results are summarized in Table 1.

Figure 2 presents absorption and fluorescence spectra upon excitation with 460 nm light of chloroform solutions of CS1, CS2, and CS3 CdSe QRs. With the increased size of the particles both absorption and fluorescence peaks shift toward longer wavelengths. The investigated CdSe QR samples CS1,

Table 1. Size Analysis of the CdSe QRs Obtained after 30 min (CS1), 20 min (CS2) and 10 min (CS3) of Synthesis

CdSe QRs	av size [nm × nm]	aspect ratio	mass [g]	molar mass [g/mol]
CS1	(3.69 ± 0.47 × 10.73 ± 1.47)	2.9	6.69×10^{-19}	4.03×10^5
CS2	(3.39 ± 0.41 × 7.96 ± 0.81)	2.5	4.19×10^{-19}	2.52×10^5
CS3	(3.11 ± 0.47 × 7.14 ± 0.86)	2.3	3.14×10^{-19}	1.89×10^5

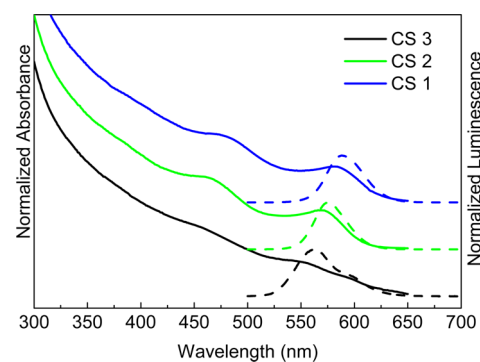


Figure 2. Absorption (solid line) and luminescence (dashed line) spectra of CdSe QRs.

CS2, and CS3 show a narrow absorption band at 590, 574, and 561 nm, respectively.

For certain applications of luminescent markers it is advantageous to excite the luminescence with light from the near-infrared (NIR) region, through multiphoton absorption. It is therefore necessary to identify the wavelength ranges in which such an excitation is the most efficient. This is why we have performed wide-wavelength studies of nonlinear absorption of the QRs and plotted those results as the two- and three-photon cross sections taken per single QR in Figure 3. We also

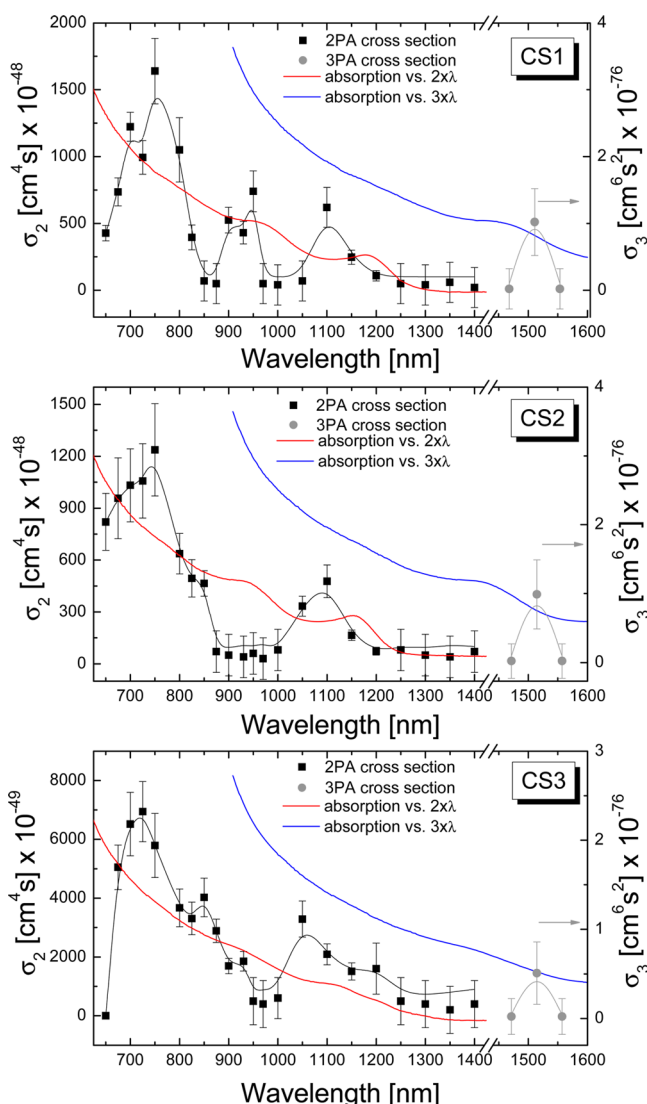


Figure 3. Dispersion of the two-photon absorption cross section σ_2 (black squares) and three-photon absorption cross-section σ_3 (gray circles), taken per an individual QR, with comparison to one-photon absorption spectra multiplied by factor 2 (red) and 3 (blue) of CdSe QRs.

compare the spectral dependence of the computed cross sections with the absorption spectra plotted vs doubled and tripled wavelength. It should be noted, however, that due to different selection rules applicable for 1PA, 2PA, and 3PA the spectra do not have to overlap. Still the comparison can suggest which order processes we can expect and inform about the nature of the observed transitions. All the investigated CdSe QRs exhibited three distinct bands in the σ_2 vs λ plot peaking at

~ 750 , ~ 1100 , and ~ 1500 nm. In order to get further insight into the mechanism of the NLO process taking place in those spectral ranges, we have performed the power dependence measurements of emission excited at 750 and 1100 nm. The results of those measurements are summarized in Figures S2–S5. Both at 750 and 1100 nm the measurements indicated two-photon character of the observed processes, which may be attributed to NLO absorption through different absorption bands of CdSe QRs. On the other hand, weak nonlinear absorption around 1500 nm is likely to be dominated by a three-photon process. It should be pointed out that it appears that in the case of the studied CdSe QRs it is possible to excite emission with light from the so-called second biological window,²⁷ through a two-photon process, which is generally more efficient than three- or even four-photon processes usually observed in this spectral ranges for some other luminescent markers.²⁸ This feature of CdSe QRs can be of great importance for biological species imaging applications. The most significant values of σ_2 were $\sim 16.4 \times 10^{-46}$, 13.3×10^{-46} , and $6.9 \times 10^{-46} \text{ cm}^4 \text{ s}/\text{QR}$ for the CS1, CS2, and CS3 CdSe QRs at ~ 750 , 750, and 725 nm, respectively. The measured maximum value of 164 000 GM for CdSe NRs is much bigger than the values of 66 000 and 7210 GM measured by us previously for spherical semiconducting particles with similar diameter: (4.2 nm) CdSe¹⁹ QDs and (5.0 nm) CdS²⁰ QDs, respectively. Li et al.¹¹ observed a similar two-photon absorption dependence on morphology of semiconducting CdS QDs and QRs. They found that for spherical CdS QDs the maximum two-photon absorption cross section σ_2 was 8400 GM; however, for CdS QRs with the aspect ratio of ~ 10 the two-photon absorption cross section was found to be increased up to 209 000 GM, which is an order of magnitude larger than that of CdS QDs of similar diameters. They concluded that expanding the volume of semiconducting nanocrystals may lead to the pronounced increase in the two-photon absorption coefficient. Similarly, elongating CdSe nanocrystals into rod-shaped ones can dramatically increase the linear absorption cross sections due to an increased volume.²⁹ It was also found that the two-photon absorption cross section for the cylindrical CdS QDs can be enhanced by up to 2 orders of magnitude.¹¹ The reason for this is that a lower degree of symmetry and the anisotropy induce splitting of degenerate energy states in cylindrical nanomaterials, which increases the density of energy states. An increased density of states, in turn, can increase probabilities of electron transitions, which are related to the two-photon absorption cross section.¹⁶ Xing et al.¹⁰ also demonstrated using single wavelength Z-scan (800 nm) that seeded CdSe/CdS heterostructures can possess two-photon absorption cross section up to 230 000 GM. It should be stressed that, in our case, the strong two-photon cross section was found for the CdSe QRs with much smaller aspect ratios. Furthermore, a more useful way to compare the applicability of different absorbers, in the case of both linear absorption and nonlinear absorption, is by scaling the relevant cross sections by the mass or volume of the absorber.³⁰ Thus, we compare here the values of two-photon absorption cross section σ_2 divided by the molecular weight (σ_2/M). In the case of the investigated CdSe QRs with three different aspect ratios the calculated value of σ_2/M was approximately equal and around 0.4 GM·mol/g, a value comparable to those for good organic or organometallic two-photon chromophores.^{30,31} It is consistent with the measurements of spherical QDs where merit factor of σ_2/M increases with size of the nanocrystals.

However, when compared to other semiconducting nanosized species, like CdSe or CdS QDs, this value is 4 and even 10 times higher, respectively. Such a high σ_2/M value also shows the advantage of two-dimensional form of CdSe QRs for imaging applications, when compared to the spherical counterparts. It must be also kept in mind that in imaging a single marker it is the total luminescence available from a marker that determines the brightness of the imaged spot, so the relevant parameters are the total nonlinear absorption cross section, the luminescence quantum yield, and also the resistance of the marker to bleaching (determining the number of luminescence photons available from the marker before it is bleached).³² Those features are advantageous for inorganic luminophores, making the investigated CdSe QRs potential candidates for replacing organic dyes in NLO imaging techniques.

TCSPC is limited to the measurements of the lifetime of radiative excited states of the QRs like $1S_e$ with the lifetimes in order of few to tens of nanoseconds. Typical quantum yields of the CdSe QDs is in range of ~5 to ~30%, and the remaining energy is dissipated in nonradiative processes with the rate constant lower than for photoluminescence. One of the techniques allowing to probe the short-lived nonradiative states is a degenerate transient absorption, which measures the lifetime of the excited state by measuring the decay of the absorption instead of fluorescence. By the use of the femtosecond laser we could measure transient absorption decay in the range of picoseconds at 560 and 800 nm in the regime of one- and two-photon absorption, respectively. The femtosecond transient absorption decays measured in one-photon degenerate pump–probe regime for various size CdSe QRs showed bleaching of the one-photon absorption (increase of transmittance) and were all quite similar as shown in Figure 4. The results are summarized in Table 2. The decays were

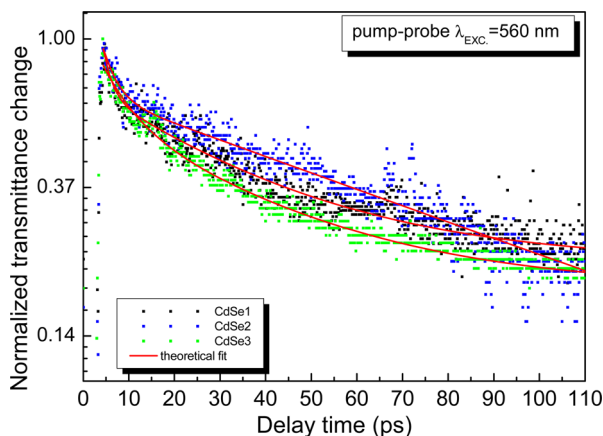


Figure 4. Femtosecond pump–probe experiment with 560 nm excitation and probing (black: CS1; blue: CS2; green: CS3; red: theoretical fits).

analyzed using a two-exponential model for all the investigated samples. The decay of the bleaching signal shows the existence of two regions with different time constants: a fast initial stage with the time constant of about a couple of picoseconds, followed by a slower decay on the order of several tens of picoseconds (Table 2). The fast component is too short to be explained by direct electron–hole recombination between quantized electron and hole states. It is therefore more likely to be due to depopulation of the lowest electron quantized states occurring via surface-defect-related states. Other work

Table 2. Comparison between the Exciton Relaxation Dynamics of the Different States in CdSe QRs Measured Using Pump–Probe and TCSPC Techniques

experiment	sample	τ_1 [ps]	τ_2 [ps]
pump–probe $\lambda_{\text{exc}} = 560 \text{ nm}$	CS1	1.88 ± 0.17	34.80 ± 0.82
	CS2	2.94 ± 0.25	88.04 ± 3.96
	CS3	6.20 ± 0.37	35.97 ± 1.06
pump–probe $\lambda_{\text{exc}} = 800 \text{ nm}$	CS1		$\tau = 0.152 \pm 0.004$
	CS2		$\tau = 0.155 \pm 0.007$
	CS3		$\tau = 0.140 \pm 0.009$
laser autocorrelation $\lambda_{\text{exc}} = 800 \text{ nm}$	BBO crystal		$\tau = 0.145 \pm 0.006$
	TCSPC $\lambda_{\text{exc}} = 460 \text{ nm}$	$8.14 \times 10^3 \pm 0.06 \times 10^3$	$26.10 \times 10^3 \pm 0.08 \times 10^3$
		$12.62 \times 10^3 \pm 0.05 \times 10^3$	$42.68 \times 10^3 \pm 0.16 \times 10^3$
	CS3	$2.60 \times 10^3 \pm 0.03 \times 10^3$	$19.44 \times 10^3 \pm 0.06 \times 10^3$

has shown that the fast decay times increase for the QRs with smaller sizes.³³ This phenomenon has been attributed to the high activity of the surface in the CdSe particles which increases with the surface-to-volume ratio. The surface states start to play a key role while the surface-to-volume ratio is increasing (0.9 nm^{-1} in our case), but for bigger QRs surface states are usually also still active.³⁴ However, their relative contribution to the decay is much smaller. The above kinetic results are consistent with the study of Mohamed et al.³⁵ They attributed these results to a consequence of the volume-induced deformation effect and also to the geometry-induced one. Decreasing the symmetry and increasing the anisotropy effect lead to changing of the degeneracy and splitting of the excited states of semiconductor nanostructures of cylindrical or ellipsoidal shapes. Another important and possible mechanism for nonradiative carrier losses in QDs is multiparticle Auger recombination (AR). AR is a process in which the e–h recombination energy is not emitted as a photon but is transferred to a third particle (an electron or a hole) that is excited to a higher energy state. Auger recombination has a relatively low efficiency in bulk semiconductors,³⁶ but in QDs, the AR rate is greatly enhanced. This has been attributed to enhanced Coulomb interactions in QDs as well as to the relaxation of the momentum conservation rule.³⁷ The AR process in QDs is much faster than radiative recombination. In PbSe QDs, for example, the AR lifetime is ~100 ps while the radiative recombination lifetime is ~800 ns.³⁸

Figure 5 shows degenerate pump–probe absorption transients for excitation at 800 nm. The resulting curves show a transient transmittance minimum (induced absorption) that appears to have no longer time tail, and thus it should be interpreted as due to instantaneous two-photon absorption. Indeed, the best fits to Gaussian curves summarized in Table 1 show no evident difference with the behavior of an autocorrelation curve recorded using SHG in a BBO crystal. The results shown in Figure 5 confirm that the absorption process measured by the Z-scan technique at 800 nm is a simultaneous two-photon process proceeding via an intermediate virtual state in the band gap. The degenerate two-photon pump–probe measurements provide a useful indicator of the dynamics of the excitation due to the fact that any relatively long-lived intermediate state that could potentially act as a path for the two-photon or a higher-order process would

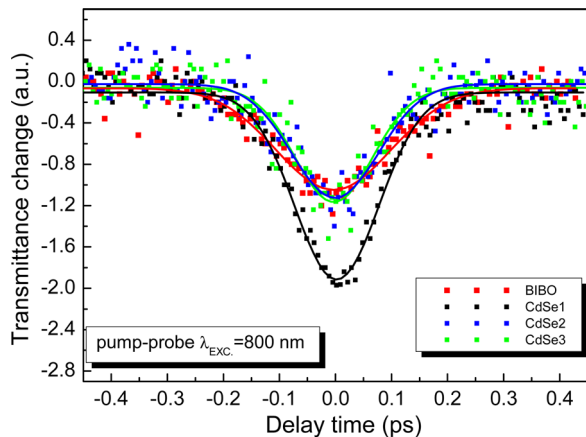


Figure 5. Degenerate transient absorption using femtosecond pump–probe experiment with 800 nm excitation and probing (black: CS1; blue: CS2; green: CS3; red: BBO crystal; solid lines: theoretical fits).

be evident in the form of a deviation from the theoretical Gaussian trace. There are no detectable wings in the pump–probe signal on the femtosecond time scale. This is agreement with the fact that Z-scan measurement in conjunction with the two-photon-induced photoluminescence signal vs power of the input excitation at $\lambda_{\text{exc}} = 750$ nm (see Supporting Information) confirms that the process involves two photons in the investigated spectral region.

In Figure 6, the fluorescence decay profiles of colloidal CdSe QRs with various sizes are shown. All spectra exhibit

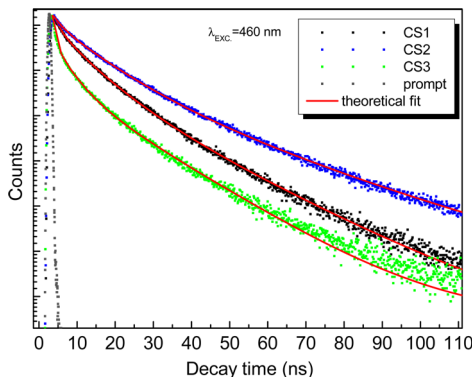


Figure 6. Room temperature fluorescence intensity decays of CdSe QRs on excitation with 460 nm (black: CS1; blue: CS2; green: CS3; gray: prompt; red: theoretical fits).

biexponential decay behavior described by $I = A_1 \exp(-t/t_1) + A_2 \exp(-t/t_2) + I_0$. A fast decay lifetime of 8–12 ns is caused by the recombination of delocalized excitons in the internal core/volume states and a slow time constant of 19–42 ns varies with different surface modifications attributed to the localized excitons in the surface state. There is no clear dependence observed between quantum rod diameter and fluorescence lifetime. The photoluminescence amplitude values of the shorter- (A_1) and the longer-lifetime (A_2) components are also size-independent with mean values of 19×10^{-3} – 24×10^{-3} for A_1 and 4.3×10^{-3} – 6.8×10^{-3} for A_2 . The ratio of the A_1 and A_2 amplitudes depends on the quality of QRs surfaces. The larger the value of A_2 (related to the longer-lifetime component), the better the surface condition (fewer the surface defects), and the larger the role of surface-related emission.³⁹

SUMMARY

In this work a comprehensive wide-wavelength range study of NLO properties of CdSe colloidal QRs has been presented. The most pronounced NLO absorption was detected in the range from 700 to 850 nm, where two-photon absorption may be expected to play a major role; however, strong two-photon absorption is also seen in the second biological transmission window. The maximum value of the two-photon absorption cross section σ_2 was found to be 164 000 GM at 750 nm, an order of magnitude larger than that of CdSe QDs of similar diameters and corresponding to 4-fold enhancement of the normalized cross section σ_2/M with respect to the QDs. This shape dependence of the NLO properties requires more in-depth studies. Indeed, even in the case of spherical QDs there has been some confusion whether the increase of the size of QDs leads to increase or decrease of the normalized two-photon absorption cross section.^{19,40} It appears now that at least in some QDs and for a certain range of QD sizes the size effect leads to the increase of σ_2/M with the diameter of the QDs. In the case of nonspherical nanoparticles the interpretation needs to take into account that the observed quantity is actually $\langle \sigma_2 \rangle$ which is the orientationally averaged cross section of the nanoparticles. Apparently, the increase of the averaged cross section with transforming of a spherical nanoparticle into an elongated one can only be explained if the increase of the component of cross section tensor corresponding to two-photon absorption of photons polarized along the long axis of the nanoparticle more than compensates for the decreases taking place for the two perpendicular directions.

Pump–probe experiments carried out in one-photon excitation range ($\lambda_{\text{exc}} = 560$ nm), and fluorescence kinetics studies have brought information on the excited state dynamics that underlines the possible importance of the nanoparticles surface states. On the other hand, degenerate femtosecond transient absorption experiments carried out in two-photon excitation range ($\lambda_{\text{exc}} = 800$ nm) have shown that, indeed, the dominant absorption process observed is the simultaneous absorption of two photons via an intermediate virtual state.

In conclusion, we have demonstrated that CdSe QRs possess the essential nonlinear optical features required, for example, in nonlinear imaging or liquid crystal nanoscience.⁴¹ Not many possible combinations of one-dimensional materials with shape and surface functionalities have yet been examined independent of the liquid crystal host phase. This study provides a foundation for the development of two-photon polarization fluorescence microscopy systems for the advanced optical imaging using enhanced two-photon absorption cross section together with the polarization-selective excitation feature of rodlike semiconductor nanoparticles.¹² Thus, more consideration should be given to nonlinear optical properties of semiconducting anisotropic nanosystems.

ASSOCIATED CONTENT

Supporting Information

Scheme of the pump–probe experimental setup, two-photon-induced luminescence of CdSe QRs, and raw Z-scan traces together with theoretical fits. This material is available free of charge via the Internet at <http://pubs.acs.org>.

AUTHOR INFORMATION

Corresponding Author

*E-mail: marek.samoc@pwr.edu.pl (M.S.).

Notes

The authors declare no competing financial interest.

ACKNOWLEDGMENTS

We acknowledge support from the National Science Centre under Grant DEC-2012/05/B/ST5/00256 and by a statutory activity subsidy from the Polish Ministry of Science and Higher Education for the Faculty of Chemistry of Wroclaw University of Technology as well as from the Foundation of Polish Science under START 2013 and WELCOME programmes.

REFERENCES

- (1) Hu, R.; Yong, K. T.; Roy, I.; Ding, H.; Law, W. C.; Cai, H. X.; Zhang, X. H.; Vathy, L. A.; Bergey, E. J.; Prasad, P. N. Functionalized Near-Infrared Quantum Dots for in Vivo Tumor Vasculature Imaging. *Nanotechnology* **2010**, *21*, 145105.
- (2) Ma, W. L.; Swisher, S. L.; Ewers, T.; Engel, J.; Ferry, V. E.; Atwater, H. A.; Alivisatos, A. P. Photovoltaic Performance of Ultrasmall Pbse Quantum Dots. *ACS Nano* **2011**, *5*, 8140–8147.
- (3) Petryayeva, E.; Algar, W. R.; Medintz, I. L. Quantum Dots in Bioanalysis: A Review of Applications across Various Platforms for Fluorescence Spectroscopy and Imaging. *Appl. Spectrosc.* **2013**, *67*, 215–252.
- (4) Panda, A. B.; Glaspell, G.; El-Shall, M. S. Microwave Synthesis of Highly Aligned Ultra Narrow Semiconductor Rods and Wires. *J. Am. Chem. Soc.* **2006**, *128*, 2790–2791.
- (5) Kan, C. X.; Zhu, X. G.; Wang, G. H. Single-Crystalline Gold Microplates: Synthesis, Characterization, and Thermal Stability. *J. Phys. Chem. B* **2006**, *110*, 4651–4656.
- (6) Xu, H.; Wang, W.; Zhu, W.; Zhou, L. Synthesis of Octahedral CuS Nanocages via a Solid-Liquid Reaction. *Nanotechnology* **2006**, *17*, 3649–3654.
- (7) Scher, E. C.; Manna, L.; Alivisatos, A. P. Shape Control and Applications of Nanocrystals. *Philos. Trans. R. Soc. London, A* **2003**, *361*, 241–255.
- (8) Olesiak-Banska, J.; Gordel, M.; Kolkowski, R.; Matczyszyn, K.; Samoc, M. Third-Order Nonlinear Optical Properties of Colloidal Gold Nanorods. *J. Phys. Chem. C* **2012**, *116*, 13731–13737.
- (9) Cassette, E.; Mahler, B.; Guigner, J.-M.; Patriarche, G.; Dubertret, B.; Pons, T. Colloidal Cdse/Cds Dot-in-Plate Nanocrystals with 2d-Polarized Emission. *ACS Nano* **2012**, *6*, 6741–6750.
- (10) Xing, G.; Liao, Y.; Wu, X.; Chakrabortty, S.; Liu, X.; Yeow, E. K. L.; Chan, Y.; Sum, T. C. Ultralow-Threshold Two-Photon Pumped Amplified Spontaneous Emission and Lasing from Seeded CdSe/Cds Nanorod Heterostructures. *ACS Nano* **2012**, *6*, 10835–10844.
- (11) Li, X.; van Embden, J.; Chon, J. W. M.; Gu, M. Enhanced Two-Photon Absorption of Cds Nanocrystal Rods. *Appl. Phys. Lett.* **2009**, *94*, 103117.
- (12) Rothenberg, E.; Ebenstein, Y.; Kazes, M.; Banin, U. Two-Photon Fluorescence Microscopy of Single Semiconductor Quantum Rods: Direct Observation of Highly Polarized Nonlinear Absorption Dipole. *J. Phys. Chem. B* **2004**, *108*, 2797–2800.
- (13) He, G. S.; Tan, L.-S.; Zheng, Q.; Prasad, P. N. Multiphoton Absorbing Materials: Molecular Designs, Characterizations, and Applications. *Chem. Rev.* **2008**, *108*, 1245–1330.
- (14) Samoc, M.; Matczyszyn, K.; Nyk, M.; Olesiak-Banska, J.; Wawrzynczyk, D.; Hanczyc, P.; Szeremeta, J.; Wielgus, M.; Gordel, M.; Mazur, L.; et al. Nonlinear Absorption and Nonlinear Refraction: Maximizing the Merit Factors. *Proc. SPIE* **2012**, *8258*, 82580V-1.
- (15) Padilha, L. A.; Fu, J.; Hagan, D. J.; Van Stryland, E. W.; Cesar, C. L.; Barbosa, L. C.; Cruz, C. H. B.; Buso, D.; Martucci, A. Frequency Degenerate and Nondegenerate Two-Photon Absorption Spectra of Semiconductor Quantum Dots. *Phys. Rev. B* **2007**, *75*, 075325.
- (16) Feng, X.; Ji, W. Shape-Dependent Two-Photon Absorption in Semiconductor Nanocrystals. *Opt. Express* **2009**, *17*, 13140–13150.
- (17) Peng, P.; Milliron, D. J.; Hughes, S. M.; Johnson, J. C.; Alivisatos, A. P.; Saykally, R. J. Femtosecond Spectroscopy of Carrier Relaxation Dynamics in Type II CdSe/CdTe Tetrapod Heteronanostructures. *Nano Lett.* **2005**, *5*, 1809–1813.
- (18) Tsen, K. T. Ultrafast Dynamics in Wide Bandgap Wurtzite Gan. *Ultrafast Phys. Processes Semicond.* **2001**, *67*, 109–149.
- (19) Nyk, M.; Wawrzynczyk, D.; Szeremeta, J.; Samoc, M. Spectrally Resolved Size-Dependent Third-Order Nonlinear Optical Properties of Colloidal CdSe Quantum Dots. *Appl. Phys. Lett.* **2012**, *100*, 041102.
- (20) Szeremeta, J.; Nyk, M.; Wawrzynczyk, D.; Samoc, M. Wavelength Dependence of Nonlinear Optical Properties of Colloidal CdS Quantum Dots. *Nanoscale* **2013**, *5*, 2388–2393.
- (21) Peng, Z. A.; Peng, X. G. Nearly Monodisperse and Shape-Controlled CdSe Nanocrystals via Alternative Routes: Nucleation and Growth. *J. Am. Chem. Soc.* **2002**, *124*, 3343–3353.
- (22) Samoc, M.; Samoc, A.; Luther-Davies, B.; Humphrey, M. G.; Wong, M. S. Third-Order Optical Nonlinearities of Oligomers, Dendrimers and Polymers Derived from Solution Z-Scan Studies. *Opt Mater.* **2003**, *21*, 485–488.
- (23) Sheik-Bahae, M.; Said, A. A.; Wei, T. H.; Hagan, D. J.; Van Stryland, E. W. Sensitive Measurement of Optical Nonlinearities Using a Single Beam. *IEEE J. Quantum Electron.* **1990**, *26*, 760–769.
- (24) Correa, D. S.; De Boni, L.; Misoguti, L.; Cohenoschi, I.; Hernandez, F. E.; Mendonca, C. R. Z-Scan Theoretical Analysis for Three-, Four- and Five-Photon Absorption. *Opt. Commun.* **2007**, *277*, 440–445.
- (25) Sutherland, R. L. *Handbook of Nonlinear Optics*; Marcel Dekker: New York, 2003.
- (26) Zhao, L.; Pang, Q.; Ge, W.; Wang, J. Investigating the Growth Mechanism of Cdse Nano-Tetrapods. *Integr. Ferroelectr.* **2012**, *137*, 98–104.
- (27) Nyk, M.; Kumar, R.; Ohulchanskyy, T. Y.; Bergey, E. J.; Prasad, P. N. High Contrast in Vitro and in Vivo Photoluminescence Bioimaging Using near Infrared to near Infrared up-Conversion in Tm³⁺ and Yb³⁺ Doped Fluoride Nanophosphors. *Nano Lett.* **2008**, *8*, 3834–3838.
- (28) Albota, M.; et al. Design of Organic Molecules with Large Two-Photon Absorption Cross Sections. *Science* **1998**, *281*, 1653–1656.
- (29) Htoon, H.; Hollingsworth, J. A.; Malko, A. V.; Dickerson, R.; Klimov, V. I. Light Amplification in Semiconductor Nanocrystals: Quantum Rods Versus Quantum Dots. *Appl. Phys. Lett.* **2003**, *82*, 4776–4778.
- (30) Schwich, T.; Cifuentes, M. P.; Gugger, P. A.; Samoc, M.; Humphrey, M. G. Electronic, Molecular Weight, Molecular Volume, and Financial Cost-Scaling and Comparison of Two-Photon Absorption Efficiency in Disparate Molecules (Organometallic Complexes for Nonlinear Optics. 48) - a Response to "Comment on 'Organometallic Complexes for Nonlinear Optics. 45. Dispersion of the Third-Order Nonlinear Optical Properties of Triphenylamine-Cored Alkynylruthenium Dendrimers.' Increasing the Nonlinear Response by Two Orders of Magnitude". *Adv. Mater.* **2011**, *23*, 1433–1435.
- (31) Larson, D. R.; Zipfel, W. R.; Williams, R. M.; Clark, S. W.; Bruchez, M. P.; Wise, F. W.; Webb, W. W. Water-Soluble Quantum Dots for Multiphoton Fluorescence Imaging in Vivo. *Science* **2003**, *300*, 1434–1436.
- (32) Nyk, M.; Wawrzynczyk, D.; Parjaszewski, K.; Samoc, M. Spectrally Resolved Nonlinear Optical Response of Upconversion Lanthanide-Doped NaYF₄ Nanoparticles. *J. Phys. Chem. C* **2011**, *115*, 16849–16855.
- (33) Klimov, V. I.; McBranch, D. W.; Leatherdale, C. A.; Bawendi, M. G. Electron and Hole Relaxation Pathways in Semiconductor Quantum Dots. *Phys. Rev. B* **1999**, *60*, 13740–13749.
- (34) Kudrawiec, R.; Nyk, M.; Syrek, M.; Podhorodecki, A.; Misiewicz, J.; Strek, W. Photoluminescence from Gan Nanopowder: The Size Effect Associated with the Surface-to-Volume Ratio. *Appl. Phys. Lett.* **2006**, *88*, 181916.
- (35) Mohamed, M. B.; Burda, C.; El-Sayed, M. A. Shape Dependent Ultrafast Relaxation Dynamics of CdSe Nanocrystals: Nanorods vs Nanodots. *Nano Lett.* **2001**, *1*, 589–593.

- (36) Klimov, V. I. Mechanisms for Photogeneration and Recombination of Multiexcitons in Semiconductor Nanocrystals: Implications for Lasing and Solar Energy Conversion. *J. Phys. Chem. B* **2006**, *110*, 16827–16845.
- (37) Pietryga, J. M.; Zhuravlev, K. K.; Whitehead, M.; Klimov, V. I.; Schaller, R. D. Evidence for Barrierless Auger Recombination in PbSe Nanocrystals: A Pressure-Dependent Study of Transient Optical Absorption. *Phys. Rev. Lett.* **2008**, *101*, 217401.
- (38) Wehrenberg, B. L.; Wang, C. J.; Guyot-Sionnest, P. Interband and Intraband Optical Studies of PbSe Colloidal Quantum Dots. *J. Phys. Chem. B* **2002**, *106*, 10634–10640.
- (39) Wang, X. Y.; Qu, L. H.; Zhang, J. Y.; Peng, X. G.; Xiao, M. Surface-Related Emission in Highly Luminescent CdSe Quantum Dots. *Nano Lett.* **2003**, *3*, 1103–1106.
- (40) Padilha, L. A.; Nootz, G.; Olszak, P. D.; Webster, S.; Hagan, D. J.; Van Stryland, E. W.; Levina, L.; Sukhovatkin, V.; Brzozowski, L.; Sargent, E. H. Optimization of Band Structure and Quantum-Size-Effect Tuning for Two-Photon Absorption Enhancement in Quantum Dots. *Nano Lett.* **2011**, *11*, 1227–1231.
- (41) Stamatoiu, O.; Mirzaei, J.; Feng, X.; Hegmann, T. Nanoparticles in Liquid Crystals and Liquid Crystalline Nanoparticles. *Liq. Cryst.: Mater., Des. Self-Assembly* **2012**, *318*, 331–393.